Applied Energy 173 (2016) 134–140

Contents lists available at ScienceDirect

Applied Energy

journal homepage: www.elsevier.com/locate/apenergy

An online method for lithium-ion battery remaining useful life estimation using importance sampling and neural networks

Ji Wu, Chenbin Zhang, Zonghai Chen *

Department of Automation, University of Science and Technology of China, Hefei 230027, PR China

HIGHLIGHTS

- An online RUL estimation method for lithium-ion battery is proposed.
- RUL is described by the difference among battery terminal voltage curves.
- A feed forward neural network is employed for RUL estimation.
- Importance sampling is utilized to select feed forward neural network inputs.

ARTICLE INFO

Article history:
Received 30 January 2016
Received in revised form 7 April 2016
Accepted 10 April 2016
Available online 12 April 2016

Keywords:
Remaining useful life
Charge process
Neural networks
Importance sampling

ABSTRACT

An accurate battery remaining useful life (RUL) estimation can facilitate the design of a reliable battery system as well as the safety and reliability of actual operation. A reasonable definition and an effective prediction algorithm are indispensable for the achievement of an accurate RUL estimation result. In this paper, the analysis of battery terminal voltage curves under different cycle numbers during charge process is utilized for RUL definition. Moreover, the relationship between RUL and charge curve is simulated by feed forward neural network (FFNN) for its simplicity and effectiveness. Considering the nonlinearity of lithium-ion charge curve, importance sampling (IS) is employed for FFNN input selection. Based on these results, an online approach using FFNN and IS is presented to estimate lithium-ion battery RUL in this paper. Experiments and numerical comparisons are conducted to validate the proposed method. The results show that the FFNN with IS is an accurate estimation method for actual operation.

1. Introduction

Due to global energy crisis and environmental pollution, the past decade has witnessed the rapid development of new energy technologies such as Electric Vehicles (EVs), Hybrid Electric Vehicles (HEVs) and Microgrids. As a power source with high energy–density, low pollution and long service life, lithium-ion battery has been widely used in a large amount of new energy systems [1–4]. Throughout the life span of a battery, its electrical property would change with battery RUL which can be regarded as the length of time from present time to the end of useful life [5]. As shown in Refs. [6,7], the safety and stability alterations of the battery would occur as well when battery RUL changes. Therefore, an accurate RUL estimation for lithium-ion battery which can help predict the battery performance variance is necessary in order to get a more scientific battery management method, a longer battery service life and a safer battery system.

Batteries would have different electrical properties, such as battery charge/discharge performance, total available capacity, peak power and so on, under different RULs. In the past 5 years, several descriptions have been utilized to characterize battery RUL. Miao et al. [8] applied an exponential growth model to fit lithium-ion battery capacity degradation curves, because capacity could gradually decrease with various aging and failure process. A sum of two exponential functions of discharge cycles were applied to model the battery capacity fade as well by He et al. [9] based on the analysis of lithium-ion battery data. Furthermore, resistance can serve as a health indicator for describing the RUL of lithium-ion batteries. Eddahech et al. [10] used a single parameter identified from Electrochemical Impedance Spectroscopy (EIS) tests, which refer to the impedance real-part at a defined frequency, to identify the battery RUL. A battery RC model was built in Kim's work [11] where capacity fade and resistance deterioration were obtained by cell characterization test data and used for battery

* Corresponding author.
E-mail address: chenzh@ustc.edu.cn (Z. Chen).

http://dx.doi.org/10.1016/j.apenergy.2016.04.057
0306-2619/

health condition indication. However, the definition of RUL using one or two battery parameter values may not be robust enough and may be lopsided. To address this issue, six influential factors were considered based on the evaluation of the battery performance characteristics, analyses on their disparities, and opinions of the experts to characterize RUL in Ref. [12]. A model fused an empirical exponential and a polynomial regression model to track the battery's degradation trend over its cycle life based on experimental data analysis is proposed in Ref. [13]. He et al. [14] described the battery aging state by several battery state of charges (SoCs) since battery with different aging states would have different SoC-OCV (open circuit voltage) curves. However, it is difficult to obtain precise OCVs in actual application. Accordingly, a reasonable definition for battery RUL is indispensable for practical operation.

On the basis of a rational battery RUL definition, a prediction algorithm is also quite necessary for RUL estimation. State estimation algorithms, like unscented Kalman filter (UKF), particle filter (PF), unscented particle filter (UPF), have been utilized for real-time prediction of battery RUL. Zheng et al. [15] employed a relevance vector regression method to simulate battery degradation. Then UKF was utilized to estimate the battery parameters for predicting RUL recursively. Similarly, PF was used for predicting RUL and time until end of discharge voltage of a lithium-ion battery in Ref. [16]. In their papers, PF was verified to have a more accurate prediction performance over UKF based on three lithium-ion battery models. Miao et al. [8] used UPF algorithm to obtain prediction results of lithium-ion batteries RUL based on a degradation model which can predict the actual RUL with an error less than 5%. RUL prediction based on machine learning tools has also been widely studied. Considering the impacts of different values of ambient temperature and discharge current, a naive Bayes (NB) model is proposed for the prediction of battery RULs under different operating conditions in Ref. [17]. A classification and regression model for RUL was built based on the critical features using Support Vector Machine (SVM) in Ref. [18] and the goal of accurate RUL prediction was achieved by using Support Vector Regression (SVR). An optimized relevance vector machine (RVM) algorithm to improve the accuracy and stability of RUL estimation and to provide an uncertainty representation for the resulting RUL estimates was presented by Liu et al. [19].

However, since (1) these advanced nonlinear filters and machine learning techniques, such as UPF in Ref. [8], SVM in Ref. [18] and RVM in Ref. [19], generally have high demands for hardware support, it is very hard to apply these algorithms in a micro controller unit (MCU) in actual battery management systems (BMS) for RUL estimation online. For example, as a binary classifier and also a non-parametric model, there may be large numbers of support vectors in SVM when it is applied to estimate RUL. This disadvantage is resulting in longer times for computation and makes SVM predominantly used as an offline tool [20]. (2) Some variables for RUL definition are hard to measure in actual operations, such as battery capacity [8,11], electrochemical impedance spectroscopy [10], and open circuit voltage [14]. The measurements of these variables require either specific equipment or particular charge/discharge schedule which make it hard to obtain the required variables. Thus the above methods may be inadequate for lithium-ion RUL estimation online.

In this paper, the RUL of lithium-ion battery is described by charge process and battery terminal voltage curve to make this characterization robust and reasonable. Batteries under different RULs would have different charge and discharge performance, which may lead to the variation of the shapes of charge and discharge curves. Afterward, FFNN with fixed hidden neurons is employed to simulate the relation between battery charge curves at constant current and battery RUL. A suitable number of hidden neurons helps to reduce hardware cost and makes the FFNN realizable to predict RUL for actual operation. In addition, IS is used for FFNN input selection to reduce the number of input neurons reasonably while also reconstitute the terminal voltage curve accurately. Then, the RUL can be estimated online by a set of weight and bias values which make up the FFNN and are stored in the MCU of BMS.

The rest of the paper is organized as follows. In Section 2, battery charge process in actual application is introduced. On the basis of this general routine, the description and definition for lithium-ion battery RUL is discussed. The FFNN and IS are introduced in Section 3. Afterward, FFNN with different hidden neuron numbers are compared in Section 4. Meanwhile, in order to evaluate the proposed FFNN with IS, comparison is accomplished as well.

2. Description and definition of RUL

Batteries would have different performance in different life states or ages. Based on this, a RUL definition is proposed in this paper.

2.1. Battery charge and discharge process in actual operation

There are three status of battery in actual practice: charge, discharge and rest. Under the influence of the rapidly changing current passing through batteries, the external and internal parameters are hard to measure or calculate accurately during the discharge process. In the stage of rest, battery parameters are generally constant or changing slowly, which would lead to a difficult estimation of internal battery parameters since they can't be calculated based on the amount of indistinctive data. However, batteries usually have a peaceable charge process in which the necessary external electrical performance can be easily measured because the charge process is controllable to battery management system. Hence, several internal battery parameters, such as battery direct current internal resistance and battery open circuit voltage, can be calculated or estimated during charging.

In this paper, the experimental IFP1865140-12Ah type lithium-ion battery which is widely used in EVs and Microgrids is developed by Hefei GuoXuan High-Tech Power Energy CO. LTD of China. Generally, charge process consists of two subprocesses in actual operation: constant current (CC) and constant voltage (CV). As shown in Fig. 1, the red[1] line is charge current curve which is constant $C/2$ (A rate of C/n is the equal of a full charge or discharge in n hours.) before battery terminal voltage reaches the cut-off voltage of 3.65 V. Afterward, battery is charged by a constant voltage of 3.65 V with a decreasing current and stops charging when the current became $C/100$. Battery terminal voltage of this IFP1865140 type lithium-ion battery that clearly indicates the severe nonlinearity is plotted in blue.

2.2. RUL description based on charge curve

It is known that the internal parameters of the battery are influenced by its RUL, and would be reflected by its external electrical performance. The battery should be replaced when it moves toward the end of its life due to the irreversible electrochemical degradation and poor discharge performance in practical operation. Obviously, internal electrochemical variation has effects on the external electrical performance and parameters. For example, battery impedance would impact battery terminal voltage, voltage drop and temperature rise. The terminal voltage is also affected by

[1] For interpretation of color in Figs. 1 and 4, the reader is referred to the web version of this article.

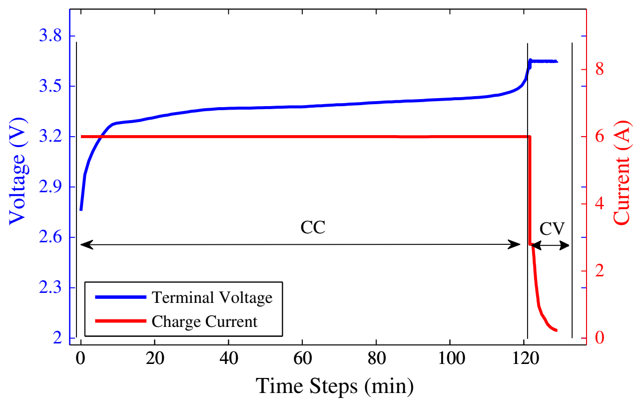

Fig. 1. Charge process in actual operation.

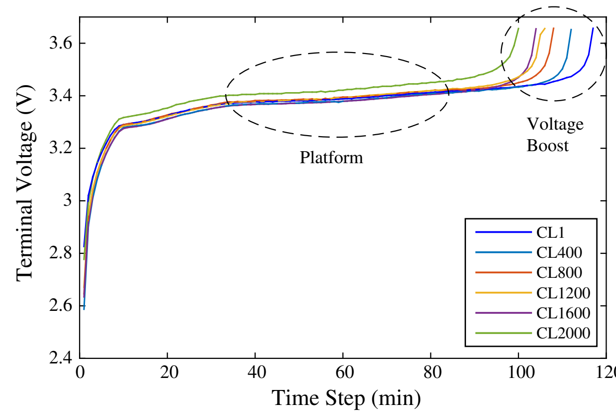

Fig. 2. Terminal voltage curves during different battery cycle numbers.

the state of charge of the battery. Thus, the variations of internal battery parameters can be calculated based on the measurement of external battery parameters. By analogy, battery RUL and health condition likewise have relationships with some measurable battery parameters.

The terminal voltage curve during charge process is applied to reflect battery RUL in this paper. Some of the reasons for using this method can be expatiated as follows. (1) As stated in Section 2.1, battery terminal voltage can be measured easily and accurately during practical battery charge process because of the mild characteristic of this process. (2) The battery would have diverse properties which can impact the performance of charge and discharge process when battery RUL varies. Accordingly, battery under different cycle numbers would have different internal property and external performance, and then lead to different terminal voltages and curve shapes during charging. This is proved by Fig. 2 which shows the shapes of battery charge curve in CC mode under different cycle numbers. As described in Fig. 2, characteristics like voltage of the platform, duration of platform, voltage boost points (process that battery voltage reach to 3.65 V from the platform) and length of the curve are all diverse among batteries under different cycle numbers. Thereupon, an approach based on the difference in battery terminal voltage curve among batteries under different cycle numbers is proposed in this paper.

2.3. Definition of the RUL

Lithium-ion battery RUL can be expressed as follows:

$$N_{\mathrm{RUL}} = N_{\mathrm{EOL}} - N_{\mathrm{ECL}} \tag{1}$$

where N_{RUL} represents the cycle number of battery RUL. N_{EOL} is the cycle number when battery comes to its end of life, which is often reached if battery actual capacity drops below 80% of its initial value in actual application. N_{ECL} is the equivalent circle life (ECL) of the battery. It is obvious that a battery has a polytropic charge/discharge current rate in actual operation. N_{ECL} is applied to formulate the cycle life via actual operation into cycle life under experiment in which battery is charged with 0.5 C and discharged with 1 C under 25 °C.

N_{EOL} is achieved by the experiment of more than 2000 charge and discharge cycles taken with the same type of batteries. As for the lithium-ion batteries studied in this paper, N_{EOL} is equal to 2063 according to the experiment data. Therefore, in order to predict N_{RUL}, an approach for N_{ECL} estimation is required and will be introduced in Section 3.

3. Methodology

3.1. Feed forward neural network

There are no explicit quantitative formulas for relationship description between the RUL and lithium-ion battery terminal voltage curves during the charge process or relationship between ECL and the curves. The relationship between battery voltage curves and battery cycle number is very difficult to perceive owing to the complex electrochemical reactions and mechanism inside the battery during its lifetime.

In order to obtain N_{ECL} which does not have a detailed expression, FFNN is applied in this work. FFNN is widely used as a machine learning method in statistical model because of its facile realization and ability for nonlinear simulation [21,22]. In this paper, a 3-layers FFNN consisting of input layer, hidden layer and output layer is proposed. Moreover, a Levenberg Marquardt (LM) based gradient descent back propagation algorithm is utilized in training the FFNN. It is expected that battery cycle life could be estimated when the network parameters are determined from the training process. The structure of this FFNN is shown in Fig. 3.

To diminish the difficulty of neural network training and improve the accuracy of estimation result, the training data of FFNN should reflect the difference in the voltage curves among batteries under different cycle numbers, and the input should represent the voltage curves during the whole CC charge subprocess exactly. Thus, battery terminal voltages during CC charge subprocess which were selected by IS are set as the inputs of the FFNN and battery equivalent circle life is the output. Moreover, the number of the neurons in FFNN's input layer is set to 11 with the purpose of equilibrating network complexity and accuracy. The hidden layer and output layer of the proposed neural network are the processing layers with activation functions at each neuron. Furthermore, the activation functions in these two layers are both hyperbolic tangent sigmoid function, as written in Eq. (2).

$$f(u) = \frac{2}{1 + e^{-2u}} - 1 \tag{2}$$

Thus, the mathematical equation of the hidden layer of the FFNN can be expressed as in Eq. (3).

$$H_i = f\left(\sum_{i=1}^{11} V_i w_{i,j}^{\mathrm{H}} + b_j^{\mathrm{H}}\right), \quad j = 1, 2, \ldots, n \tag{3}$$

where H_i is the ith output note of the hidden layer, V_i is the input battery terminal voltage, $w^{\mathrm{H}}{}_{i,j}$ is the weight value connecting the ith input neuron and the jth hidden neuron, $b^{\mathrm{H}}{}_j$ is the threshold

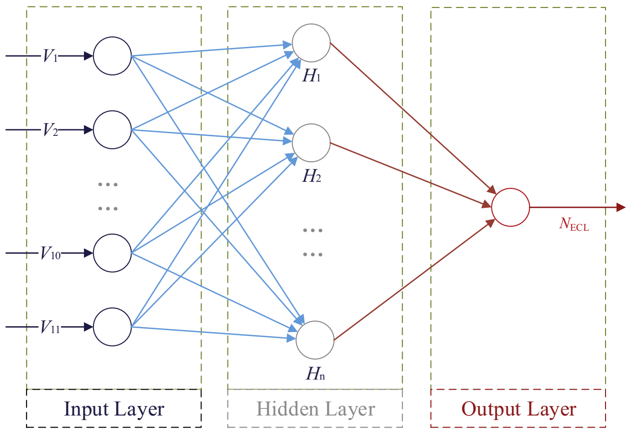

Fig. 3. Structure of feed forward neural network.

value of the jth neurons in the hidden layer, n is the number of the neurons in the hidden layer.

Subsequently, based on Eq. (3), the output of this neural network can be calculated as follows:

$$N_{\mathrm{ECL}} = f\left(\sum_{j=1}^{n} H_j w_{j,k}^{\mathrm{O}} + b_k^{\mathrm{O}}\right), \quad k = 1 \tag{4}$$

where $w^{\mathrm{O}}{}_{j,k}$ is the weight value connecting the jth hidden neuron and the kth output neuron, $b^{\mathrm{O}}{}_k$ is the threshold value of the kth neuron in the output layer, k is the number of the neuron in the output layer and k is equal to 1 in this paper since N_{ECL} is the only output of the FFNN.

Battery terminal voltages during constant current charge subprocess of each charge/discharge cycle in the experimental situation are measured and selected for network training. The values of the weight and bias in the FFNN are determined after the training process. In addition, these values can be written in the EEPROM of battery management system and makes it possible to estimate battery RUL by the FFNN during the actual operation of the EVs, HEVs and Microgrids. The equation applied to calculate battery RUL can be defined as follows:

$$N_{\mathrm{RUL}} = N_{\mathrm{EOL}} - f\left(W_{\mathrm{O}}^{\mathrm{T}} \cdot f\left(W_{\mathrm{H}}^{\mathrm{T}} \cdot V + B_{\mathrm{H}}\right) + B_{\mathrm{O}}\right) \tag{5}$$

where $W_{\mathrm{H}} = \left(w_{1,1}^{\mathrm{H}}, \ldots, w_{j,k}^{\mathrm{H}}, \ldots, w_{j,1}^{\mathrm{H}}\right)^{\mathrm{T}}$ is the weight matrix of the neurons in the hidden layer, $W_{\mathrm{O}} = \left(w_{1,1}^{\mathrm{O}}, \ldots, w_{i,j}^{\mathrm{O}}, \ldots, w_{11,n}^{\mathrm{O}}\right)^{\mathrm{T}}$ is the weight matrix of the neurons in the output layer, $V = (V_1, \ldots, V_{11})^{\mathrm{T}}$ is the input vector of the input layer, $B_{\mathrm{H}} = \left(b_1^{\mathrm{H}}, \ldots, b_j^{\mathrm{H}}\right)^{\mathrm{T}}$ is the threshold value of the neurons in the hidden layer, $B_{\mathrm{O}} = b_k^{\mathrm{O}}$ is the threshold value of the neurons in the output layer.

3.2. Importance sampling

It is obvious that there would be a large number of sampling points during 0.5 C rate CC charge process even if the sample period of battery management system is 1 s. Measured voltage data should be selected to make them possible to act as the inputs of FFNN. As shown in Fig. 2, the terminal voltage of the lithium-ion battery during CC charge process is nonlinear, especially at the beginning and the end of the process. It is also shown that the terminal voltage curve shapes of the battery in different cycle numbers are quite dissimilar. As mentioned earlier in this paper, the input of FFNN should reflect the difference in the voltage curves among batteries under different cycle numbers and represent the voltage curves during the whole CC charge subprocess exactly. IS is applied in this paper for FFNN input selecting instead of traditional uniform sampling to reduce the number of input neurons of FFNN reasonably and reconstitute the terminal voltage curve accurately.

IS [23,24] is a wildly used variance reduction technique based on Monte Carlo theory. The basic idea of IS is that certain samples would be more important than others and would have more impact on the result of signal reconstitution or rare event simulation. Thus, the main purpose of IS is to select an appropriate distribution to increase the relative frequency of these important samples. In order to make IS unbiased, the contribution of every sample is weighted by the importance function.

As shown in Fig. 4, some voltage samples in the battery CC charge curve are more important than others for curve reconstitution. These samples would have greater impacts on the shape of the voltage curve. The purpose of IS is to select 11 suitable important samples from hundreds of the terminal voltage samples. The difference in the voltage curves among batteries under different cycle numbers could be held by IS for its unbiasedness. In order to apply IS in actual operation, the key issue is to find an importance function for the voltage samples in the battery CC charge curve. Unfortunately, there are no general rules for selecting an importance function that is appropriate for all occasions.

Obviously, the samples which have a bigger terminal voltage variation make greater contributions than others to changing the shape of battery terminal voltage curve. Hence, the voltage difference between two adjacent sample points is defined as the importance function in this paper. The mathematical expression is shown as follows:

$$f_1(k) = V_k - V_{k-1} \tag{6}$$

where $f_1(k)$ is the importance function of kth voltage; V_k and V_{k-1} are the kth and $k-1$th voltage respectively.

In Fig. 4, battery terminal voltage during CC charge subprocess is the blue line, and the red one is the curve of the importance function. As a more important interval, the end of charge has values of the importance function of nearly 0.1 V which is much bigger than platform's 0 V. Hence, more samples from the end of charge will be selected as the input of FFNN. Furthermore, a non-sampling interval is defined since batteries usually are not fully discharged when charging started in the practical use. On the basis of massive actual data analysis and project application, the non-sampling interval is about from 0% to 30% SoC in this paper.

To encourage the contribution of the important samples, 8 samples are chosen from the boosting voltage interval. 3 samples are picked from the platform to make sure that the IS is unbiased. Eventually, 11 samples are selected from the regions of 80 min before end of charge to the end, such as end of charge, 1 min before the end, 2 min before the end and so on, as shown in Fig. 4. The count backwards form of time is applied to acquire the samples in order to eliminate the influence of different total charging time.

4. Experiments and analysis

With the purpose of testifying the RUL estimation method proposed in this paper, several experiments and simulations are taken. Lithium-ion battery cell voltages are measured by a battery testing system comprised of a 63640-80-80 type DC electronic load and a programmable 62006P-30-80 type DC power supply model both develop by Chroma ATE Inc. Selected IFP1865140 type batteries were developed by HeFei GuoXuan High-Tech Power Energy CO. LTD of China in this platform. MATLAB is used to simulate the experiment data in this paper.

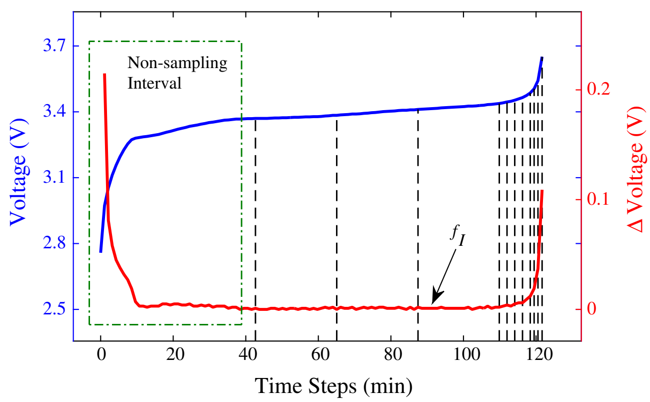

Fig. 4. Importance sampling.

4.1. FFNN with different hidden neuron numbers

In order to identify the reasonable number of FFNN hidden neurons, different hidden neuron numbers have been essayed. The threshold number is set to 60 considering the processing capacity of the MCU in BMS. Accordingly, comparison of these four networks with different hidden neuron numbers are presented. Considering the actual ambient temperature of the batteries in the real applications, the experiment data was obtained by experiments under the constant temperature of 25 °C. Furthermore, to make the result more persuasive, a FFNN with empirical number of hidden neurons, which is twice as large as the input layer and was suggested in Ref. [25] either, is employed as a comparison group.

Two sets of charge and discharge data through the whole using life, more than 2000 charge and discharge cycles, of 2 different IFP1865140 type lithium-ion batteries were applied to train and validate FFNN respectively in this paper. Inputs of the FFNN are 11 battery terminal voltages selected by IS proposed in Section 3.

The FFNN was trained by the experiment data of over 2000 cycles and tested by the other data of 2000 cycles from another battery to justify the validity of the proposed RUL estimation method. The prediction results and errors based on FFNN with different hidden neuron numbers are shown in Fig. 5(a) and (b) respectively. Moreover, the numerical result is shown in Table 1.

As shown in Table 1, FFNN with more hidden neurons would be able to have better performance. A FFNN with 50 hidden neurons would have about 55% less of MAE than the FFNN had 22 neurons. The MSE of FFNN with 20 hidden neurons is also larger than FFNN with more hidden neurons. However, the more hidden neurons contained in the network, the more computing workload imposed on MCU. To balance the demand of estimation accuracy and MCU performance, a FFNN with 40 hidden neurons is applied in the actual BMS for RUL prediction online.

4.2. Comparison of importance sampling and uniform sampling

To validate the IS, RUL estimation results of FFNN with two different battery terminal voltage reconstitution methods, IS and uniform sampling (US), which are applied to input neurons selection respectively are compared in this section. Unlike the IS, uniform sampling thinks every sample point has the same importance. Therefore, 11 points with equal sampling interval are chosen by US.

Battery RUL estimation results between FFNN using IS and US are compared. To guarantee the fairness, the compared neural networks are trained by the same experiment data, initialized by the same weights and biases. Moreover, the hidden neurons are both 40 as well. Fig. 6(a) is the comparison of estimation result, and Fig. 6(b) is the estimation error. As shown in the enlarged curves, it is clearly that FFNN utilizing IS has a better performance than the one using US. The numerical result is shown in Table 2. The FFNN-US method has a MAE of 36.3539, while the MAE of FFNN-IS is 29.4218. It is a 27.3% improvement by FFNN-IS. A less MSE is achieved by FFNN-IS as well.

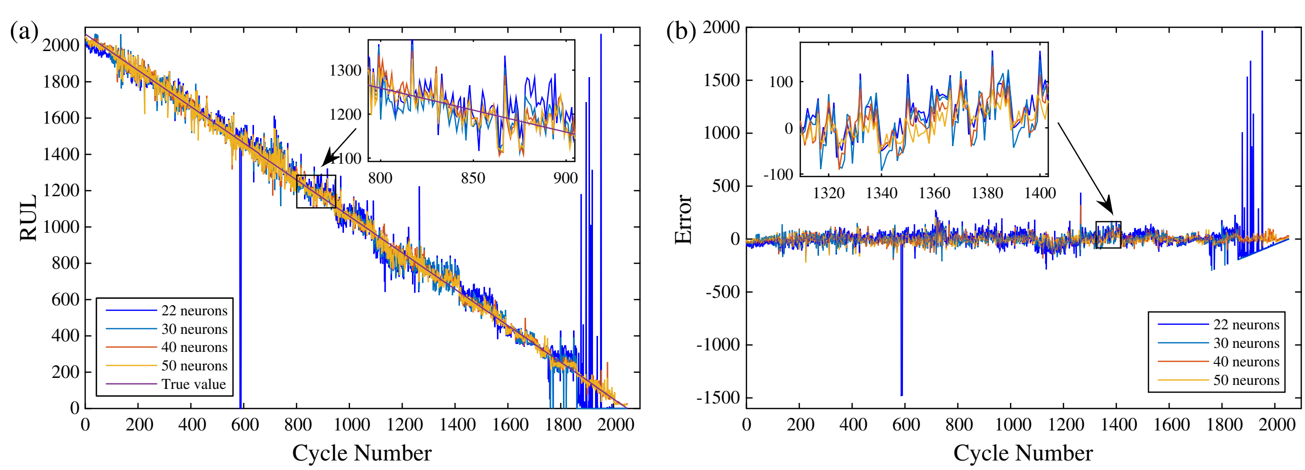

Fig. 5. Comparison of FFNN with different hidden neuron number: (a) RUL estimation results; (b) RUL estimation errors.

Table 1
Numerical results of FFNN with different hidden neuron number.

Hidden neuron number	22	30	40	50
MAE[a]	57.2056	40.7189	29.4218	25.6123
MSE[b]	1.7675e+04	3.2344e+03	1.6184e+03	1.2300e+03

[a] MAE = Mean absolute error.
[b] MSE = Mean squared error.

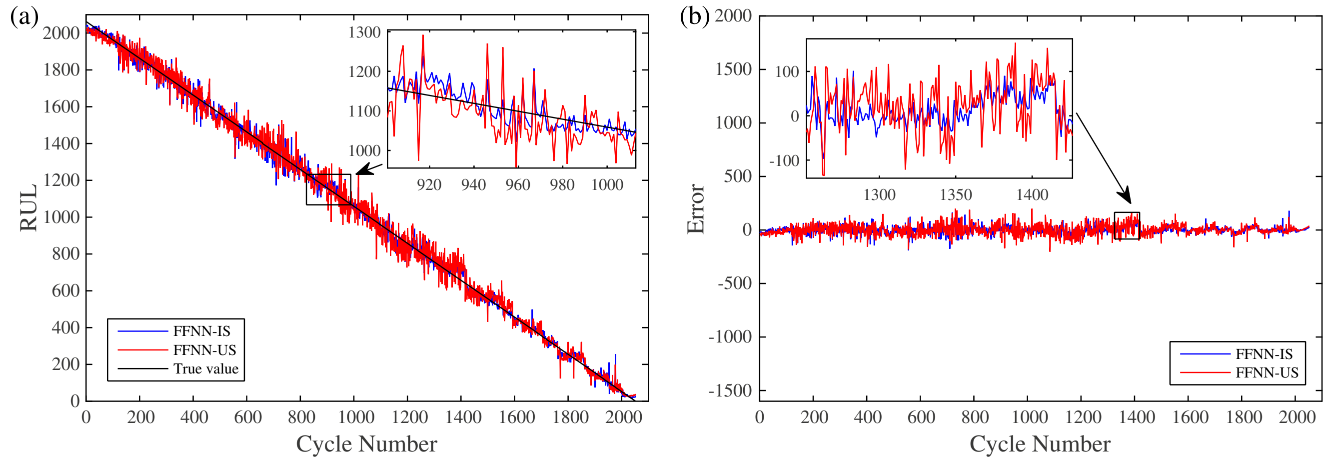

Fig. 6. Comparison of IS and US: (a) RUL estimation results; (b) RUL estimation errors.

Table 2
Numerical results of FFNN using IS and US.

Method	FFNN-IS	FFNN-US
MAE	29.4218	36.3539
MSE	1.6184e+03	2.3232e+03

The above comparisons show that the proposed FFNN using IS has a reliable battery RUL prediction performance. Meanwhile, 40 is confirmed to be a reasonable number of the hidden neurons for actual BMS application.

5. Conclusion

On the basis of RUL definition reflected by the curves of constant current charge subprocess, a lithium-ion battery RUL estimation method using FFNN and IS is presented in this paper. To predict RUL online, the hidden neuron number is set to 40 via the contrast experiment. The mean absolute error and mean square error of the proposed method in the prediction of the RUL is 29.4218 and 1.6184e+03 respectively in about 2000 cycles. In other words, the presented online approach using FFNN and IS can predict the actual RUL with an error less than 5% for practical operation. The experimental results indicate that the proposed method has a reliable RUL estimation performance for online application. Therefore, the major contributions made in this paper are listed as follows. (1) The difference in voltage curves of battery CC charge subprocess among batteries under different cycle numbers is used for RUL definition for robust consideration. (2) A FFNN with 40 hidden neurons is employed for estimating RUL online. (3) IS is utilized to select FFNN input from amount of voltage points for accurate lithium-ion charge curve reconstitution. In the future, RUL estimation for battery under different charge current rate will be studied.

Acknowledgement

This work is supported by the National Natural Science Fund of China (Grant No. 61375079). The authors would like to thank Mr. Jun Zhang and Dr. Hui Zhang for their useful suggestions.

References

[1] He Y, Liu X, Zhang C, Chen Z. A new model for State-of-Charge (SOC) estimation for high-power Li-ion batteries. Appl Energy 2013;101:808–14.
[2] Liu X, Wu J, Zhang C, Chen Z. A method for state of energy estimation of lithium-ion batteries at dynamic currents and temperatures. J Power Sources 2014;270:151–7.
[3] Wu J, Zhang C, Chen Z. A novel lithium-ion battery model for state of charge estimation under dynamic currents. In: 4th International conference on Electric Power and Energy Conversion Systems (EPECS); 2015. p. 1–6.
[4] Guan Y, Vasquez JC, Guerrero JM, Wang Y, Feng W. Frequency stability of hierarchically controlled hybrid photovoltaic-battery-hydropower microgrids. IEEE Trans Ind Appl 2015;51:4729–42.
[5] Tang S, Yu C, Wang X, Guo X, Si X. Remaining useful life prediction of lithium-ion batteries based on the wiener process with measurement error. Energies 2014;7:520–47.
[6] Wang Y, Zhang C, Chen Z. An adaptive remaining energy prediction approach for lithium-ion batteries in electric vehicles. J Power Sources 2016;305:80–8.
[7] Sun F, Xiong R, He H. Estimation of state-of-charge and state-of-power capability of lithium-ion battery considering varying health conditions. J Power Sources 2014;259:166–76.
[8] Miao Q, Xie L, Cui H, Liang W, Pecht M. Remaining useful life prediction of lithium-ion battery with unscented particle filter technique. Microelectron Reliab 2013;53:805–10.
[9] He W, Williard N, Osterman M, Pecht M. Prognostics of lithium-ion batteries based on Dempster–Shafer theory and the Bayesian Monte Carlo method. J Power Sources 2011;196:10314–21.
[10] Eddahech A, Briat O, Woirgard E, Vinassa JM. Remaining useful life prediction of lithium batteries in calendar ageing for automotive applications. Microelectron Reliab 2012;52:2438–42.
[11] Il-Song K. A technique for estimating the state of health of lithium batteries through a dual-sliding-mode observer. IEEE Trans Power Electron 2010;25:1013–22.
[12] Sun B, Jiang J, Zheng F, Zhao W, Liaw BY, Ruan H, et al. Practical state of health estimation of power batteries based on Delphi method and grey relational grade analysis. J Power Sources 2015;282:146–57.
[13] Xing Y, Ma EWM, Tsui K-L, Pecht M. An ensemble model for predicting the remaining useful performance of lithium-ion batteries. Microelectron Reliab 2013;53:811–20.
[14] He Z, Gao M, Ma G, Liu Y, Chen S. Online state-of-health estimation of lithium-ion batteries using Dynamic Bayesian Networks. J Power Sources 2014;267:576–83.
[15] Zheng X, Fang H. An integrated unscented kalman filter and relevance vector regression approach for lithium-ion battery remaining useful life and short-term capacity prediction. Reliab Eng Syst Safe 2015;144:74–82.
[16] Walker E, Rayman S, White RE. Comparison of a particle filter and other state estimation methods for prognostics of lithium-ion batteries. J Power Sources 2015;287:1–12.
[17] Ng SSY, Xing Y, Tsui KL. A naive Bayes model for robust remaining useful life prediction of lithium-ion battery. Appl Energy 2014;118:114–23.
[18] Patil MA, Tagade P, Hariharan KS, Kolake SM, Song T, Yeo T, et al. A novel multistage Support Vector Machine based approach for Li ion battery remaining useful life estimation. Appl Energy 2015;159:285–97.
[19] Liu D, Zhou J, Liao H, Peng Y, Peng X. A health indicator extraction and optimization framework for lithium-ion battery degradation modeling and prognostics. IEEE Trans Syst Man Cyber Syst 2015;45:915–28.
[20] Waag W, Fleischer C, Sauer DU. Critical review of the methods for monitoring of lithium-ion batteries in electric and hybrid vehicles. J Power Sources 2014;258:321–39.
[21] Sandberg IW. Nonlinear dynamical systems: feedforward neural network perspectives. John Wiley & Sons; 2001. p. 1–15.
[22] Dong G, Zhang X, Zhang C, Chen Z. A method for state of energy estimation of lithium-ion batteries based on neural network model. Energy 2015;90(Part 1):879–88.

[23] Sadowsky JS. A new method for Viterbi decoder simulation using importance sampling. IEEE Trans Commun 1990;38:1341–51.
[24] Biondini G. An introduction to rare event simulation and importance sampling. In: Venu Govindaraju VVR, Rao CR, editors. Handbook of Statistics. Elsevier; 2015. p. 29–68 [chapter 2].
[25] Berry MJ, Linoff G. Data mining techniques: for marketing, sales, and customer support. John Wiley & Sons, Inc.; 1997.